Analysis of strong motion records of the Cephallenian shock occurring on Sept. 17, 1972 and of its larger aftershock

J. Drakopoulos (*) – A. Roussopoulos (**)

Received on August 1st, 1973

Summary. — In the present paper the first strong motion accelerograms from the area of Greece are analysed. The general information of the main shock and the larger aftershock are also introduced. Current data processing techniques for strong motion accelerograms and modern improvements in data recovery capabilities are discussed. The analysis of the recorded strong motion accelerograms were accomplished by digital computer and the main seismic characteristics of the ground motion were obtained such as: period-frequency analysis, probability-density distribution, auto-correlation function, power spectral density, ground acceleration, velocity and displacement, response spectra etc. Some useful information about the nature of the motion of the ground have been taken from this investigation.

Riassunto. — Nella presente nota vengono analizzati per la prima volta accelerogrammi « strong motion » ottenuti in Grecia, con le relative generali informazioni sulla scossa principale e sulle repliche più forti. Vengono inoltre discussi le tecniche attuali per la trattazione dei dati da accelerogrammi « strong motion », nonchè i moderni progressi raggiunti per la reperibilità dei dati stessi. L'analisi delle registrazioni « strong motion » è stata effettuata a mezzo di elaboratore digitalizzato che ha fornito le principali caratteristiche sismiche del movimento del suolo, cioè: analisi periodo-frequenza, distribuzione probabilità-densità, funzione di auto-correlazione, spettro di potenza, accelerazione del suolo, velocità e spostamento, spettro di risposta etc... Da questa ricerca si sono avute utili informazioni sulla natura del movimento del suolo.

(*) National Observatory of Athens, Thission, Athens, Greece.
(**) National Technical University of Athens, Athens, Greece.

1. – Introduction

Seismologists and earthquake engineers except of the other fields of their sciences study the intensity of seismic waves and mainly the ground acceleration associated with these, since they are interested in the effects that earthquakes have on structures. Appraisal of these effects is possible by measuring the value of acceleration.

Strong motion instruments offer themselves for such measurements, as they generally record the acceleration associated with strong ground movements. The development of instrumentation for the detection and recording of local earthquakes by strong motion instruments began just after 1932. The first accelerogram was obtained in 1933 during the Long-Beach earthquake in California, and since then about 500 valuable records have been obtained by the U.S. Coast and Geodetic Survey of earthquakes of a destructive or potentially destructive size. About one-half of these records were obtained during the San Fernando earthquake of Febr. 9, 1971 and of these 250 records some 120 were recorded in the upper floors of high-rise buildings ([4]). Smaller numbers of records were obtained for other important earthquakes. The limited number of strong motion records which exist give us an idea of the importance of them.

Computer methods facilitate immensely the use of recorded data, their classification and the calculation and analysis of the main seismic characteristics of the ground. By modern data processing techniques the accelerograms can be integrated to produce ground velocities and displacement with a satisfactory accuracy. A digitized accelerogram cannot be integrated immediately in an attempt to determine ground velocity and displacement for the following reasons. The initial velocity and displacement and the actual zero base line for the digitized accelerogram are not known. Of these three unknowns, finding the zero base line of the accelerogram is the most important step in accelerogram data processing.

By the use of high-resolution digitization and digital filtering it is possible to remove random errors from the records to the point that integrations and differentiations can be carried out over prescribed frequency domains ([5]).

The most complete description of earthquake ground motion is the accelerogram itself which expresses the full time history of the true ground acceleration. The most simple way to have in a quantitative way the effect of an earthquake on structure is the peak horizontal ground acceleration which is readily available from the accelerogram and it is commonly thought to be closely related to the lateral forces on a structure. This is in fact the case for high-frequency systems, but for intermediate and low frequency structures, which include most buildings and engineering works, the ground acceleration is not even an approximate indication of the actual lateral earthquake forces. A better overall picture would be obtained by specifying as well the maximum ground velocity and the maximum ground displacement, as these quantities would sample respectively the intermediate frequency and the lower frequency regimes (5). If one single ground parameter must be insisted upon, it appears that the peak ground velocity would probably be the best. As has been shown by Hudson (3) this peak ground velocity is commonly used to express the damaging potential of shocks and is correlated at least roughly with the Modified Mercalli intensity.

In the present paper the first motion accelerograms from the area of Greece are analysed and compared. So some useful information about the nature of the motion of the ground have been taken from this investigation.

2. – Instrumentation

Some countries, such as U.S.A., Japan, U.S.S.R. and others with high technical knowledge and experience, have developed various types of strong-motion instruments in order to face the destructive earthquakes which occur.

The basic instrument for strong motion seismology is the strong motion accelerograph, which records three components of ground acceleration versus time. The SMAC-B type accelerograph which has been installed on Cephallenia records ground acceleration up to 1 g with a resolution of the order of 1 gal. A vertical electrodynamic starter is used which has a flat frequency from about 1-10 CPS and can be set to trigger at acceleration level above 5 or 10 gal. So the recording is made automatically when an earthquake of more than 5 gals takes place and the four subsequent large earthquakes can be recorded in the event that the seismograph cannot be inspected immediately following the large earthquake.

A simplified instrumentation network consisted of 27 seismoscopes have been installed in Western Greece. Four seismoscope records were obtained during the Cephallenian main shock at sites having varying local soil and geological conditions and so some additional ground motion distributions were ascertained as for example the attenuation of ground motion with distance can be clearly seen.

This type of seismoscope consists of a conical pendulum free to move in any horizontal direction about a pivot point which is attached to the ground. The pendulum has an undamped period of 0.75 seconds and magnetic damping of 10% critical. The two-dimensional horizontal response is marked out by a stylus on a smoked spherical watch glass. The seismoscope can be regarded as a dynamic model of typical structure and from its response, one point on the response spectrum curve is directly determined. The amplitude of the seismoscope record thus indicates the relative severity of the ground motion in the frequency range of structural interest (5). The seismoscope, of course samples the ground motion at just one frequency although the amount of damping is such that major fluctuations of response with frequency are not usually to be expected.

3. – General information of the earthquakes

At 14 hours 07 min, G.M.T. on September 17, 1972 a large earthquake occurred near the Western coast of Cephallenia Island. USCGS calculated the epicenter at 38.3°N, 20.3°E; BCIS and the seismological institute of the National Observatory of Athens calculated the same epicenter at 38.2°N, 20.4°E. The shock produced property damages in several localities, in Southwestern part of the Cephallenia island. According to official reports 108 old houses were damaged beyond repair and 53 were cracked. In addition 2 school buildings 2 churches and 2 bridges were cracked.

The rather extensive property damage only in some old buildings is attributed principally to poor construction of these buildings in the region. However the location of some of the villages on alluvium was a contributing factor in these instances. It is not our intent to elaborate further on the damage to specific buildings.

In Fig. 1, the isoseismal map of the earthquake on Mercalli-Sieberg scale is illustrated with some additional necessary seismological information. Area of felt shaking about 720,000 km^2, $r_5 = 280$ km. Macroseismic magnitude $M.M = 6.8$ and macroseismic focal depth ca 60 km. The instrumental magnitude was 6.2.

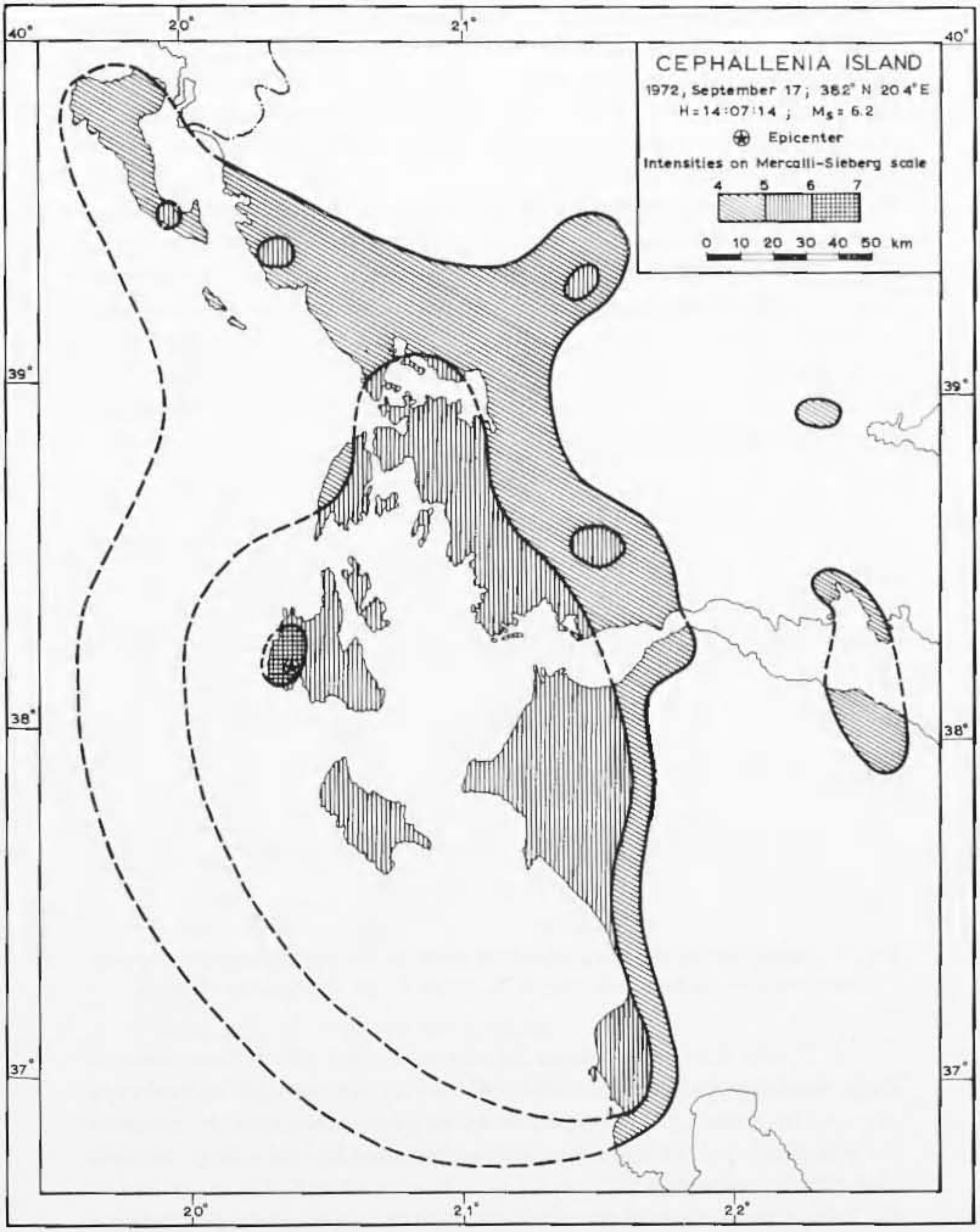

Fig. 1 – Isoseismal map of the Cephallenian main shock of September 17, 1972.

Accelerograms of the earthquake are shown in Fig. 2. These records are from a SMAC-B type strong motion seismograph installed at Argostolion (38°10'N, 20°36'E) on Cephallenia island. Calibration of the SMAC records were made and results revealed no particular defect with exception of the vertical component which failed to record distinctly.

The epicentral distance was about 30 km. It must be mentioned here that the foundation at the site of strong motion seismograph is limestone. By those records (fig. 2) the following fact became clear that the maximum acceleration directly measured by the accelerograms was 170 gals in E-W component while 130 gals was the maximum in N-S component and duration of the tremor of which amplitude exceeded more than 100 gals continued for more than 2.5 seconds in horizontal components.

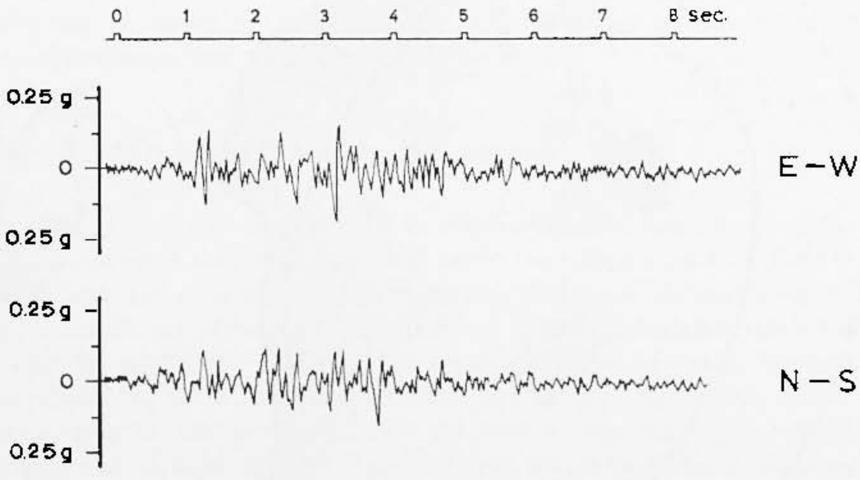

Fig. 2 – Records for the main shock of a SMAC-B type strong motion seismograph at Argostolion (38°10'N, 20°36'E) on Cephallenia Island.

A 12 mm N100°E full-scale deflection of a SR-100 Wilmot seismoscope was observed at the site of the strong motion seismograph (fig. 3). In Mesologhi (38°36'N, 21°45'E) and Zante 37°46'N, 20°56'E) the recording pen of the seismoscopes deflected by 2.5 mm in N150°E and N20°E, respectively.

Since these two lastly mentioned sites are in almost equal distances from the foci and in a different orientation relatively to the probable fault, we may say that the values attenuate with distance in a fairly uniform way. There is strong evidence by the distribution of the epicentres of aftershocks that the fault is in a direction NNW and if this is true, it is difficult to say if the motions were more severe perpendicular to the fault than parallel to it.

A late aftershock occured on Oct. 30 (14 h 32 min) with almost the same epicenter and magnitude of 5.5. Area of felt shaking about 180,000 km², $r_5 = 120$ km (fig. 4). Accelerograms of this aftershock by the same SMAC-B type strong motion seismograph installed at the same place are indicated in fig. 5.

This aftershock produced a N 90°E full-scale deflection of the SR-100 Wilmot seismoscope assigned at Argostolion by 7 mm.

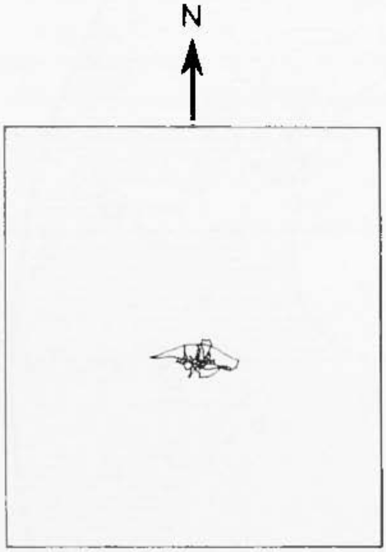

Fig. 3 – A 12 mm N100°E full-scale deflection of a SR-100 Wilmot seismoscope installed at the site of the strong motion seismograph.

4. – Analysis of the accelerograms

In figs 6a and 6b probability-density distribution of the E-W and N-S accelerogram are shown correspondingly.

In figs 7a and 7b are shown the power spectral density plots of the E-W and N-S components. As it is clear from these figures the predominant frequencies in the two horizontal components were 2 cps for E-W and 4 cps for N-S component. Thus the spectra at the site are concentrated around the periods 0.5 sec in E-W component and 0.25 sec in N-S component.

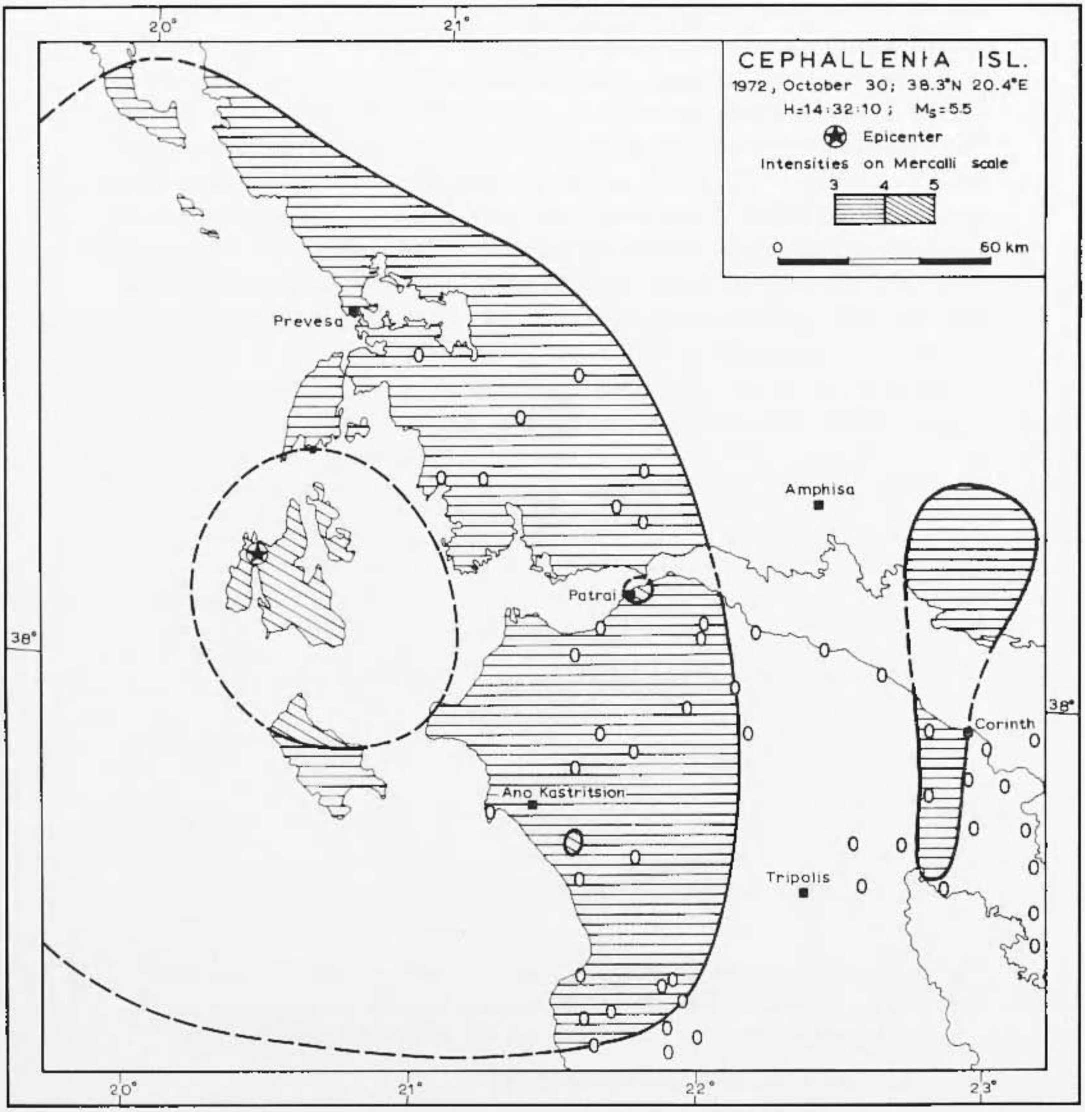

Fig. 4 – Isoseismal map of the late aftershock of October 30, 1972.

So it is clear that these is not coincidence of the predominant periods of the earthquake in both horizontal components. In figs 8a and 8b you can see the modified power spectral density of the E-W and N-S components correspondingly.

The Fourier spectral density functions of the two components are indicated in the figs 9a and 9b for the E-W and N-S components correspondingly. From the fig. 9a it is concluded that the period for main max. is 0.50 sec while two other secondary maximum are in periods 0.30 sec and 0.15 sec. From the fig. 9b it is clear that the period for main max. is 0.25 sec, and spectra are also concentrated around the periods 0.40 sec and 0.15 sec.

We obtained the same plots for the larger aftershock. What it is worth to mention from the results is that the predominant periods are comparatively smaller in the corresponding components during the aftershock. The ratio of the main shock predominant period to that of the aftershock for E-W component was 1.34 and for N-S component was 1.47.

Another important observation for the aftershock is the absence of well expressed secondary maximum for other periods. That is mainly due to the small duration of the record.

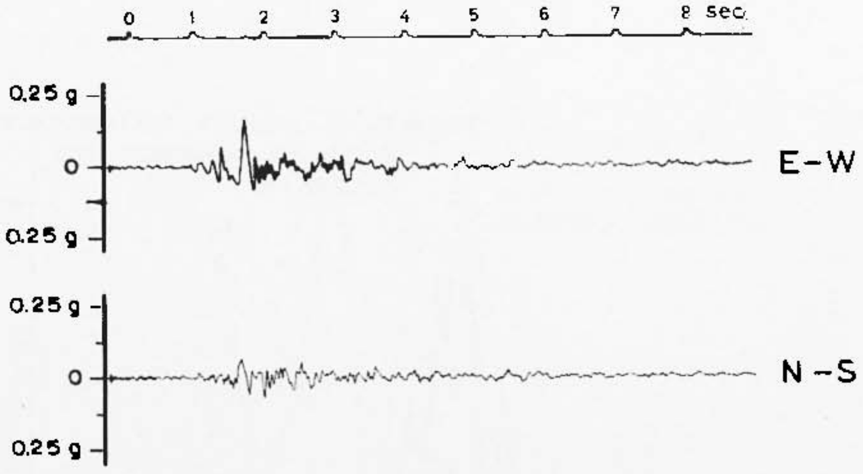

Fig. 5 – Records for the late aftershock of a SMAC-B strong motion seismograph at Argostolion (38°10′N, 20°36′E) on Cephallenia Island.

5. – Response spectrum

The response spectra of earthquake ground motion is defined as the plot of the maximum response of a series of a single degree of freedom, linear, viscously damped oscillators to a prescribed ground

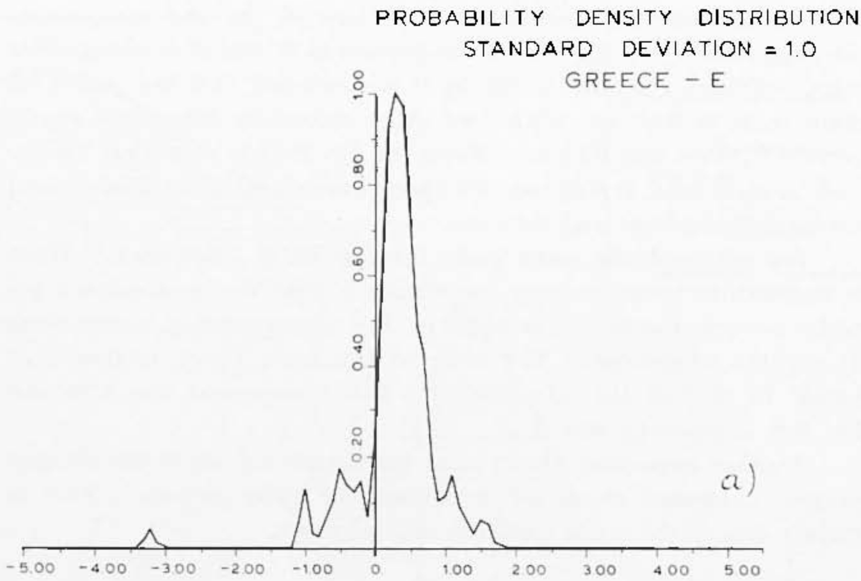

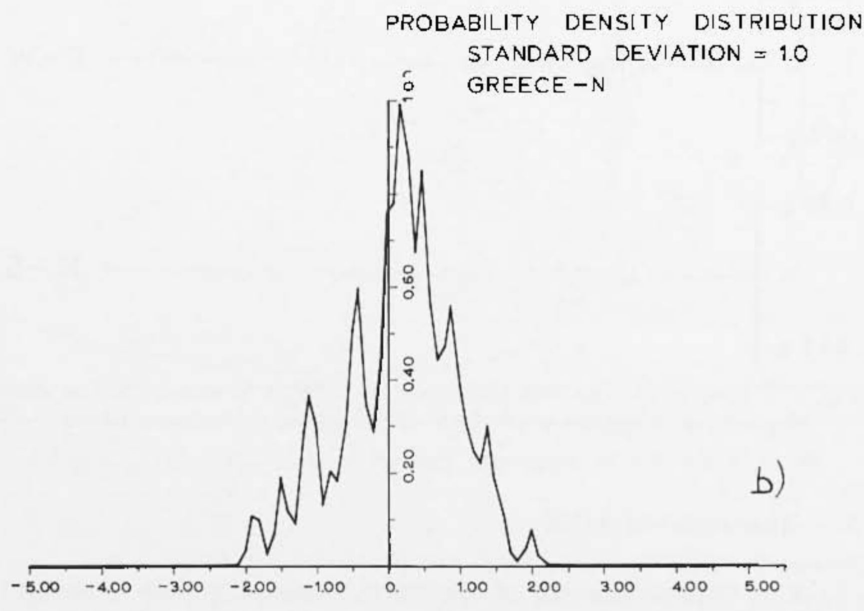

Fig. 6 – Probability density distribution of the main shock for the E-W (6a) and N-S (6b) accelerograms.

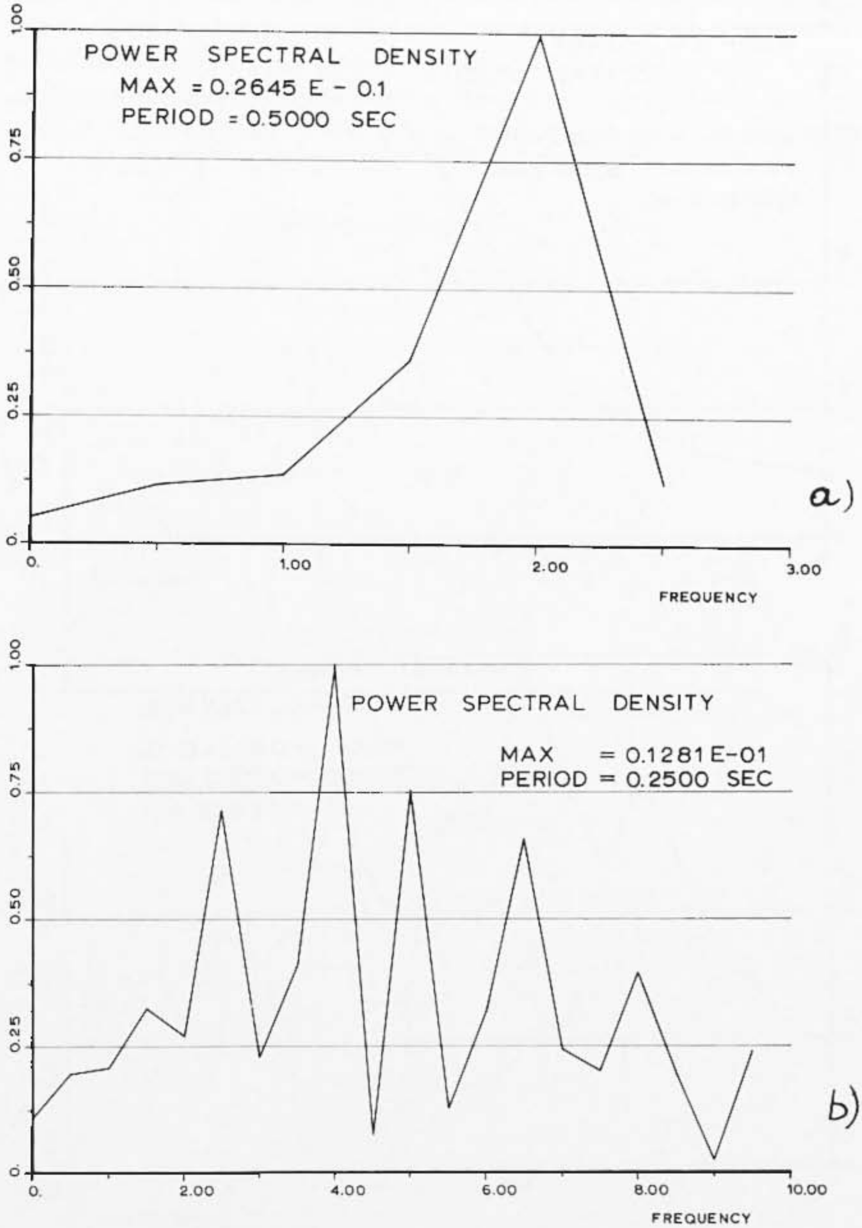

Fig. 7 – Power spectral density of the main shock for the E-W (7a) and N-S (7b) accelerograms.

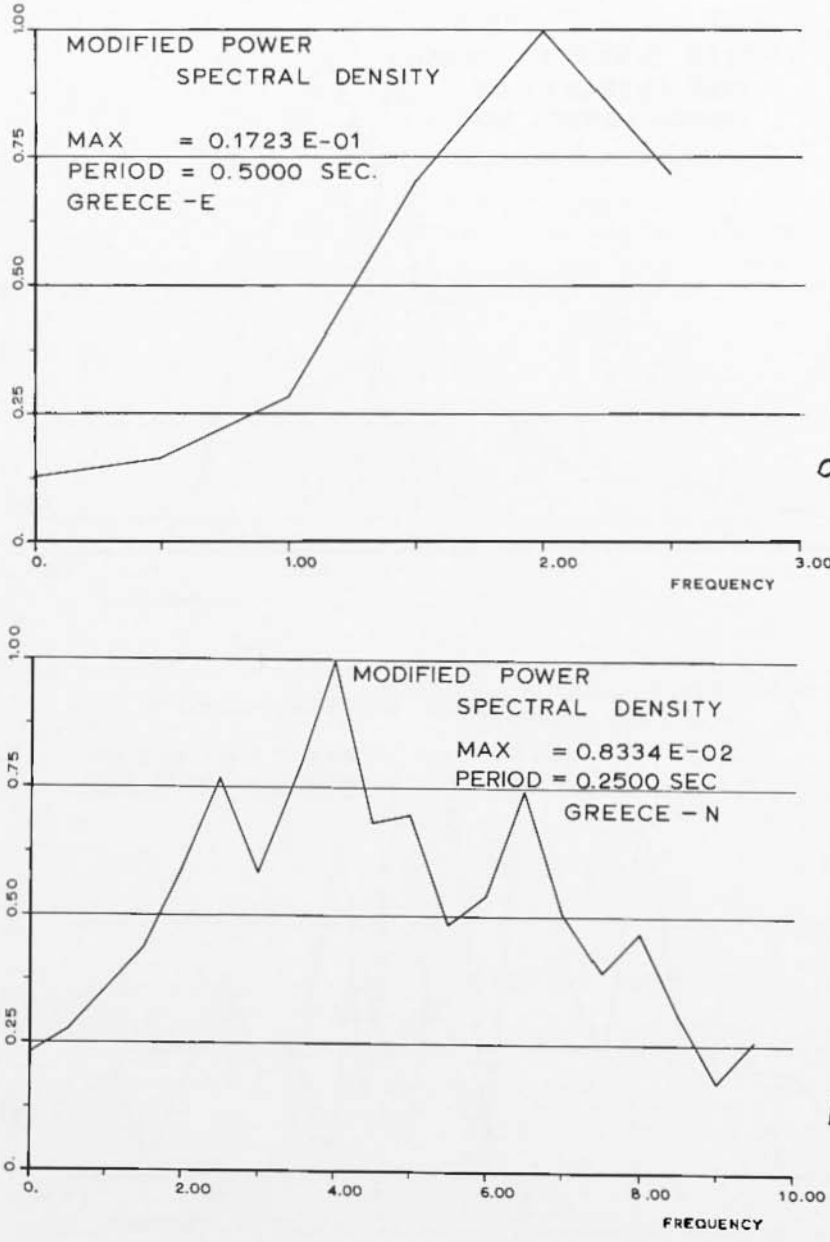

Fig. 8 – Modified power spectral density of the main shock for the E-W (8a) and N-S (8b) accelerograms.

motion, versus the natural period of the oscillator for various fractions of critical damping. The response spectra can be expressed in terms of relative displacement, relative velocity and relative or absolute acceleration. These curves provide a description of the frequency characteristics of the ground motion and give the maximum

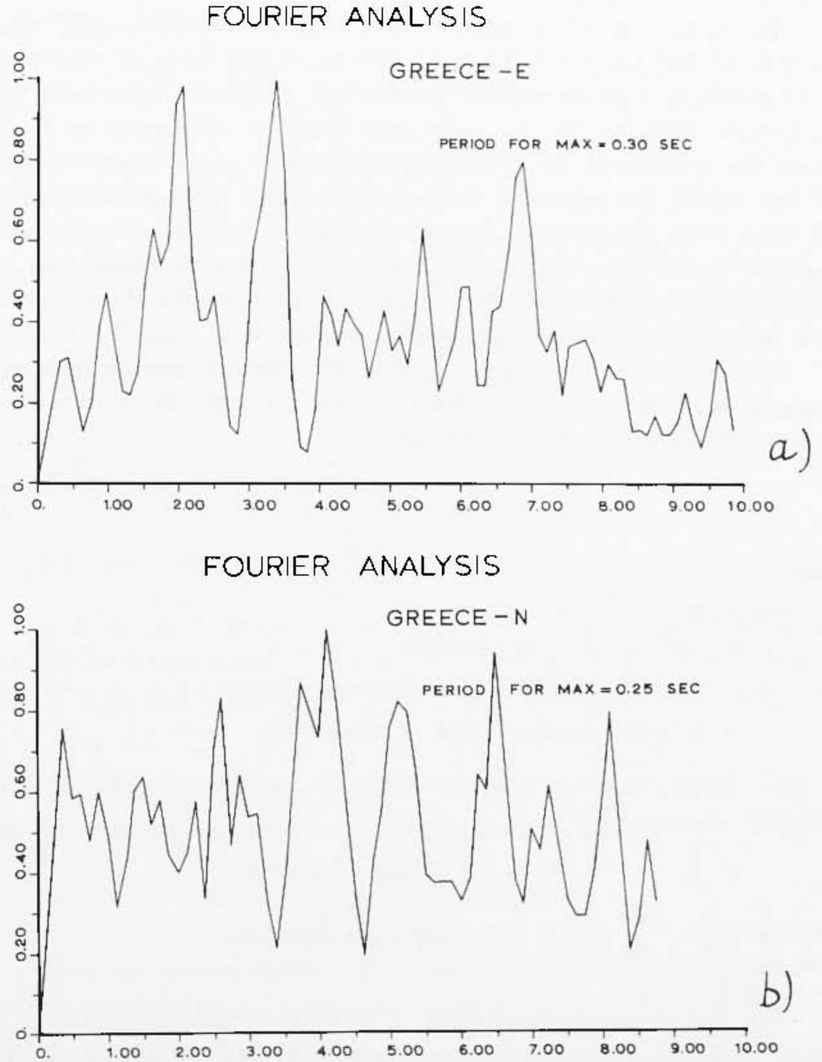

Fig. 9 – Fourier spectral density function of the main shock for the E-W (9a) and N-S (9b) accelerograms.

response of simple structures to the earthquake. By superposition of different modes of response, spectrum techniques can be applied to the design and analysis of complex structures such as multistory buildings and dams. Used in this manner the spectrum technique represents an approach intermediate between a design based on static loads and a complete integration of the equations of motion of the complex structures [2,6].

Strong-motion earthquake records have been obtained infrequently in the past and the reduction to digital form or equivalent analogue form and subsequent calculation of spectra have been performed on more or less an individual basis [6]. However, in recent years the number of strong-motion instruments in the seismic regions of the world, has increased to the point where a major earthquake in these areas will generate a large number of records. The potential volume of the data and the development of the tape-recording accelerograph indicate clearly that rapid and automated data processing and spectrum calculation procedures are needed.

The response of a single degree of freedom, linear, viscously damped system, at any instant t, to an arbitrary time dependent ground displacement u_o is given by

$$m \frac{d^2}{dt^2}(u + u_o) + C\frac{du}{dt} + Ku = 0 \qquad [1]$$

Where

m — mass.

C = viscous damping coefficient.

K = coefficient of stiffness of the system.

u = relative displacement of the mass.

$u_o(t)$ = displacement of the base from the position of rest. We can simplify equation [1] to

$$m\ddot{u} + C\dot{u} + Ku = -mg(t) \qquad [2]$$

Where $g(t) = \frac{d^2}{dt^2}(u_o)$ is the ground acceleration.

For the strong-motion records it was found that the accelerogram trace could be approximated quite closely by a series of straight line segments. In that case it is for $t_{i-1} \leqslant t \leqslant t_i$, $g(t) = a_i(t - t_{i-1}) + b_i$, where a_i, b_i, are constants of the *ith* segment.

Using this assumption it is easier and quicker using computer technique to solve the equation of motion.

By getting the ground acceleration in a digitised form equation [2] can be written as follows:

$$m \frac{d^2u}{dt^2} + C \frac{du}{dt} + Ku = -m\,[a_i\,(t - t_{i-1}) + b_i]. \qquad [3]$$

Equation [3] can be written

$$\frac{d^2u}{dt^2} + 2\lambda w_0 \frac{du}{dt} + w_0^2 u = -a_i\,(t - t_{i-1}) - b_i$$

where

$$w_0^2 = \frac{K}{m} \quad \text{and} \quad 2\lambda w_0 = \frac{C}{m}$$

By getting the solution of the equation for u (relative displacement), $\dot{u}$ (relative velocity), u_a (absolute acceleration), and with the initial conditions known i.e, $\dot{u} = u = 0$ at $t = 0$ these values can be calculated by a step by step process at any required instant.

6. – Base line correction

6.1. *Some basic assumptions*

It is assumed that the accelerogram is considered as a series of straight lines connecting each peak of it. Thus starting from the equation of a straight line passing from two points

$$y - y_1 = \frac{y_2 - y_1}{x_2 - x_1}\,(x - x_1)$$

the acceleration can be calculated (fig. 10)

$$\ddot{u}\,(t) = \frac{\ddot{u}_i - \ddot{u}_{i-1}}{t_i - t_{i-1}}\,(t_i - t_{i-1}) + \ddot{u}_{i-1}$$

Since the accelerogram is given in time-acceleration coordinates, the acceleration can be calculated at any desirable interval of time ([6]). Thus

$$\ddot{u}\,(t + \Delta t) = \frac{\ddot{u}_i - \ddot{u}_{i-1}}{t_i - t_{i-1}}\,(t + \Delta t - t_{i-1}) + \ddot{u}_{i-1} = \ddot{u}(t) + \frac{\ddot{u}_i - \ddot{u}_{i-1}}{t_i - t_{i-1}}\,\Delta t$$

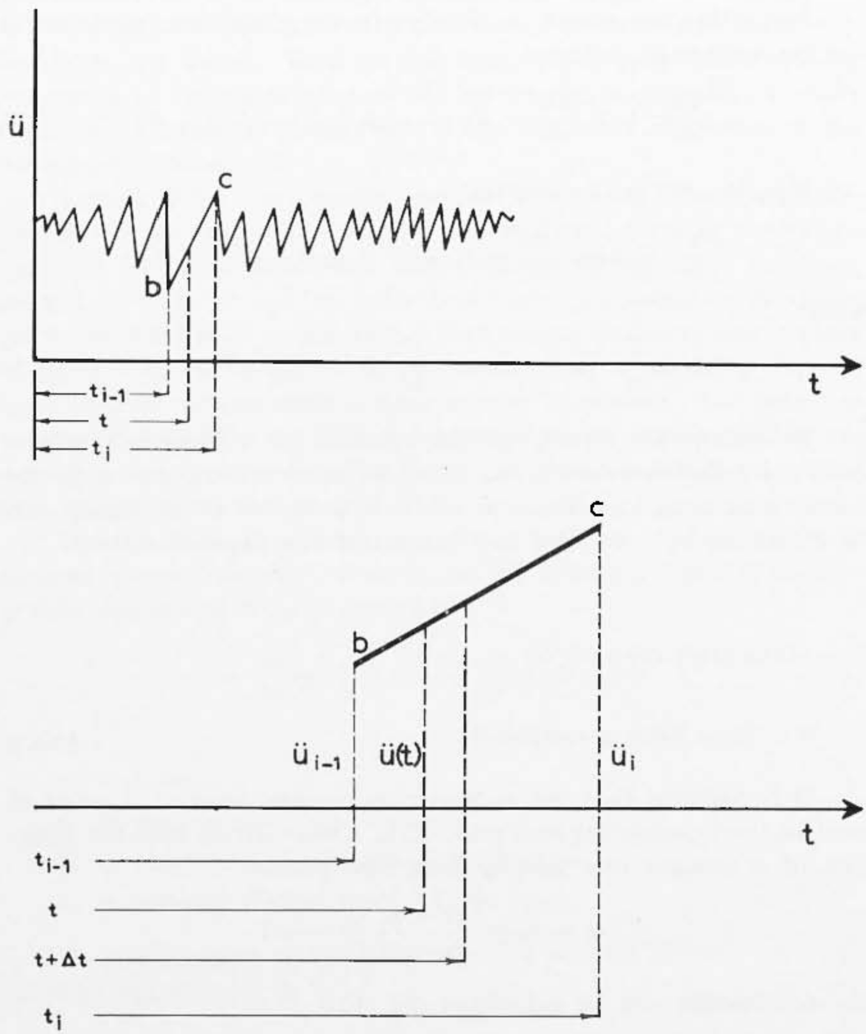

Fig. 10 – Explanation figure in time-acceleration coordinates.

According to Taylor series for a function $F(x)$

$$F(x + \Delta x) = F(x) + \frac{\dot{F}(x)\,\Delta x}{1\,!} + \frac{\ddot{F}(x)\,\Delta x^2}{2\,!} + \frac{\dddot{F}(x)\,\Delta x^3}{3\,!} + \ldots\ldots$$

For the ground velocity

$$\dot{u}(t + \Delta t) = \dot{u}(t) + \frac{u(t)\,\Delta t}{1!} + \frac{\ddot{u}(t)\,\Delta t^2}{2!} =$$

$$= \dot{u}(t) + \frac{1}{2}\,\ddot{u}(t)\,\Delta t + \frac{1}{2}\,\ddot{u}(t + \Delta t)\,\Delta t$$

And for the ground displacement

$$u(t + \Delta t) = u(t) + \frac{\dot{u}(t)\,\Delta t}{1!} + \frac{\ddot{u}(t)\,\Delta t^2}{2!} + \frac{\dddot{u}(t)\,\Delta t^3}{3!} =$$

$$= u(t) + \dot{u}(t)\,\Delta t + \frac{1}{3}\,u(t)\,\Delta t^2 + \frac{1}{6}\,u(t + \Delta t)\,\Delta t^2$$

By integration of the straight line of the acceleration we get a curve of 2nd for the velocity and by a new integration of the velocity we get a curve of 3rd for the displacement. Integration can be carried out much more accurately than differentiation, since it is easier to determine the way in which the area under a complicated curve varies with time than it would be to measure the slope of the curve.

For further increase in accuracy in the calculation of the above quantities it is necessary to apply a base-line correction to the recorded acceleration, since no base-line is available straight from the accelerogram; the base-line correction of the acceleration, influences the calculation of ground velocity and displacement.

After the calculation of the base-line correction, we can find the points where the acceleration becomes zero. These points of zero acceleration correspond to maximum values of velocity. This is very important especially for the calculation of the response spectra. We can find in this way missing values of velocity which we could not before adjusting the base line (7).

6.2. *Least-Mean-Square-Velocity Technique*

This technique introduced by Berg and Housner (1), adds a time-dependent second order polynomial ($C_0 + C_1t + C_2t^2$) to the acceleration, giving by this way to the acceleration base-line the shape of a second degree parabola. The technique makes the mean square value of the ground velocity a minimum. This is justified mainly by the feeling that most earthquake ground motions of significant time duration correspond to ground velocities which oscillate approximately symmetrically about a zero axis and approach zero velocity at the end of the earthquake. A similar condition could not be applied to the ground displacement since permanent ground displacements at the end of the earthquake could occur.

It has been shown by Hudson ([3]) that the periods introduced in the accelerogram by the parabolic base-line correction do not seriously affect the accuracy of the response spectra calculations for periods up to about 5 sec. Also the parabolic base-line does not meet all of the requirements for the standard base-line correction, because it depends largely on the record length, and the low frequency components will be treated differently from one accelerogram to another.

If u_c is the corrected acceleration and $\ddot{u}$ the uncorrected acceleration by introducing the time dependent second order polynomial we have:

$$u_c = \ddot{u} - (C_1 + 2\,C_2 t + 3\,C_3 t^2)$$

hence

$$\dot{u}_c = \dot{u} - (C_1 t + C_2 t^2 + C_3 t^3)$$

$$u_c = u - \left(\frac{1}{2}\,C_1 t^2 + \frac{1}{3}\,C_2 t^3 + \frac{1}{4}\,C_3 t^4\right)$$

where $\dot{u}_c$, $\dot{u}$ are the corrected and uncorrected ground velocities and u_c, u are the corrected and uncorrected ground displacements.

The minimization of the mean square ground velocity requires the quantity $P = \int_0^T \dot{u}_c^2\,dt$ to be minimum.

So we have

$$R = \int_0^T \dot{u} - (C_1 t + C_2 t^2 + C_3 t^3)^2\,dt \rightarrow \text{min.}$$

In accordance with the rules of partial differentiation

$$\frac{\partial R}{\partial C_1} = 0 \qquad \frac{\partial R}{\partial C_2} = 0 \qquad \frac{\partial R}{\partial C_3} = 0$$

and the final conditions are

$$\frac{T^3}{3}\,C_1 + \frac{T^4}{4}\,C_2 + \frac{T^5}{5}\,C_3 = \int_0^T \dot{u}t\,dt$$

$$\frac{T^4}{4}\,C_1 + \frac{T^5}{5}\,C_2 + \frac{T^6}{6}\,C_3 = \int_0^T \dot{u}t^2\,dt$$

$$\frac{T^5}{5}\,C_1 + \frac{T^6}{6}\,C_2 + \frac{T^7}{7}\,C_3 = \int_0^T \dot{u}t^3\,dt.$$

Assuming initial conditions of zero velocity and displacement and with $\ddot{u}$ and T known the C's values can be evaluated.

By this way the corrected values of acceleration, velocity and displacement can be calculated. The above corrected quantities provide the basis of spectral calculations which, as maximum response values can be expressed in terms of acceleration velocity and displacement for different dampings.

In figs 11a and 11b the relative displacement for different damping ratios are indicated for E-W and N-S components. In figs 12a and 12b you can see, for the same damping ratios, the relative velocities of the two components and in figs 13a and 13b the absolute accelerations. All these curves are valid for the main shock.

We applied the same technique to the accelerograms obtained during the larger aftershock and we have families of curves for the two horizontal components and the same damping ratios for the relative displacements, relative velocities and absolute accelerations.

These spectra are important for engineering purposes, since the acceleration spectra enable us to obtain the higher and lower frequencies of ground movement and the velocity spectra are related to energy values which can be used for design purposes.

7. – Conclusions

From the records of the main shock by seismoscopes we may conclude that the values attenuate with distance in a fairly uniform way. It was impossible to investigate if the motions were more severe perpendicular to the fault than parallel to it.

From the power spectral density plots it was found for the main shock that the predominant frequencies were 2 cps for E-W and 4 cps for N-S component.

The ratio of the main shock predominant period to that of the late aftershock for E-W component was found 1.34 and for N-S component was found 1.17. The absence of well expressed secondary maximum, for other period sthan the predominant one, for the late aftershock was attributed to the small duration of the record.

Since the initial velocity and displacement and the actual zero base-line for the digitized accelerogram are not known in order to produce ground velocities and displacements with a satisfactory ac-

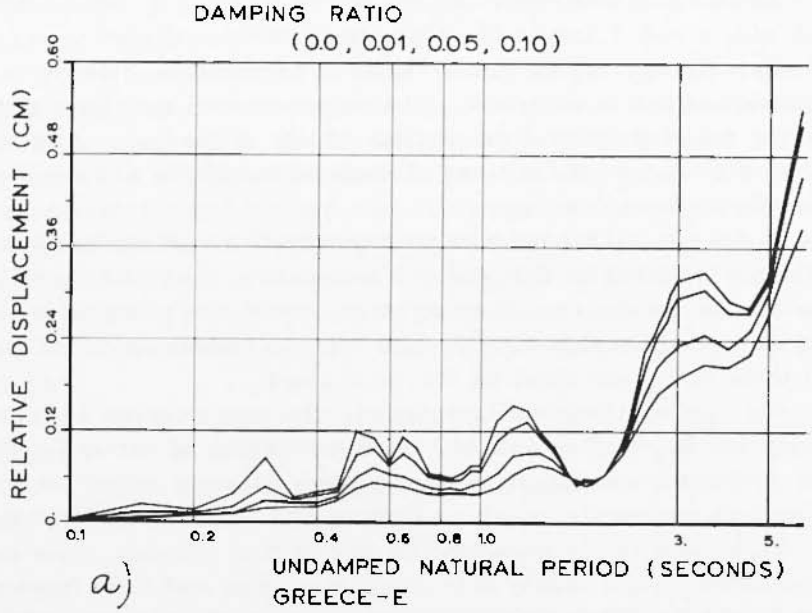

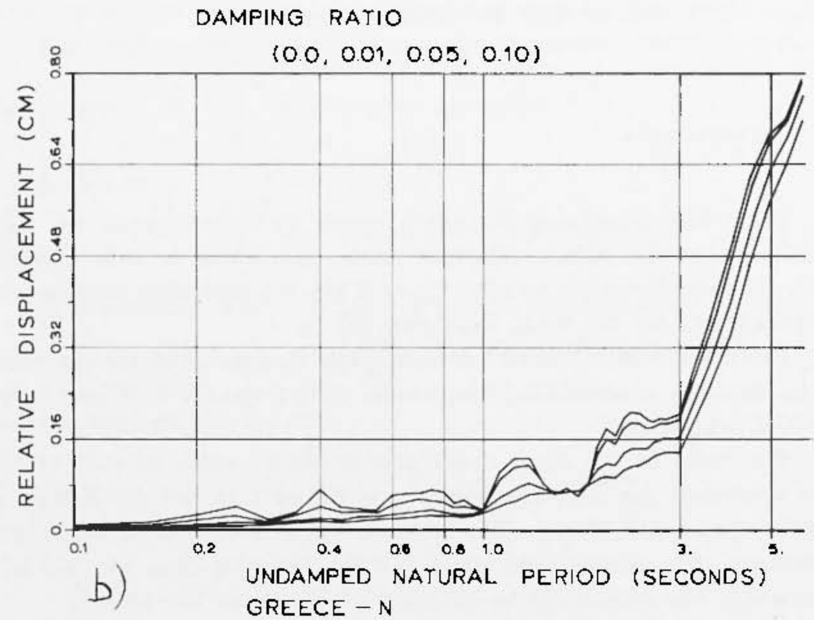

Fig. 11 – Relative displacements versus period and different damping ratios of the main shock for E-W (11a) and N-S (11b) components.

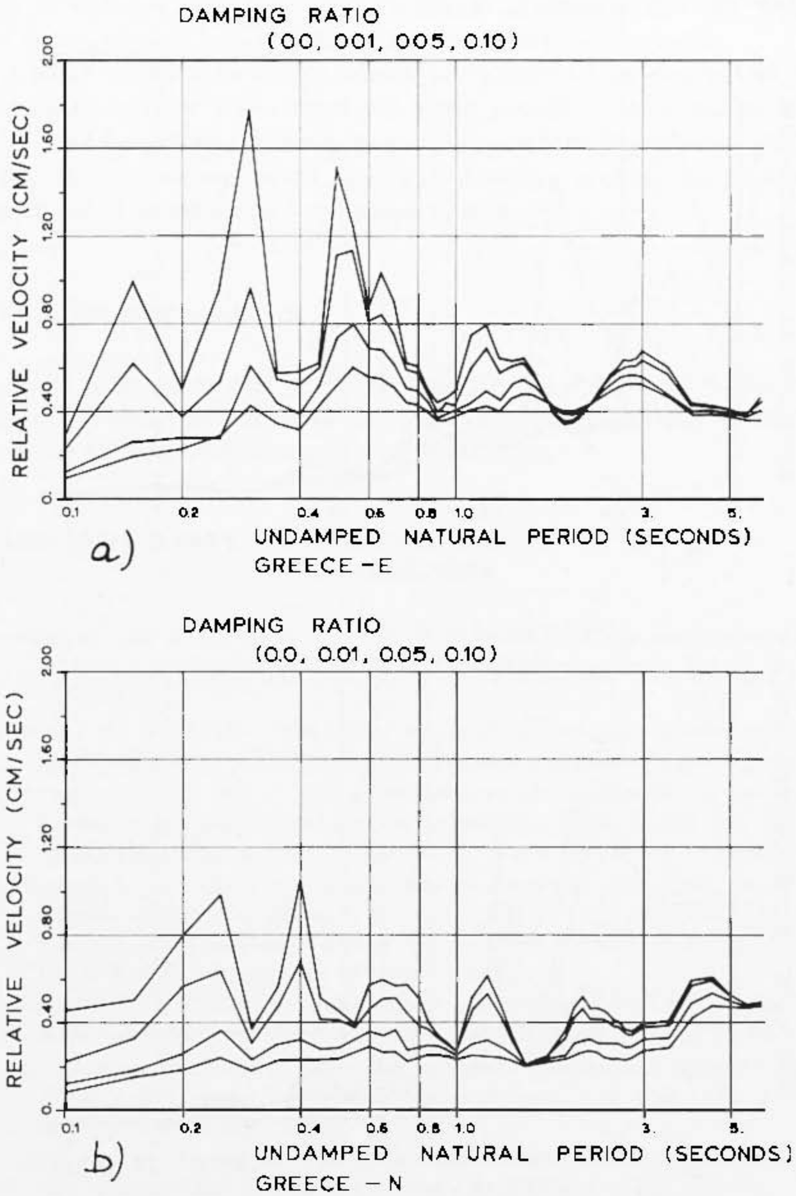

Fig. 12 – Relative velocities versus period and different damping ratios of the main shock for E-W (12a) and N-S (12b) components.

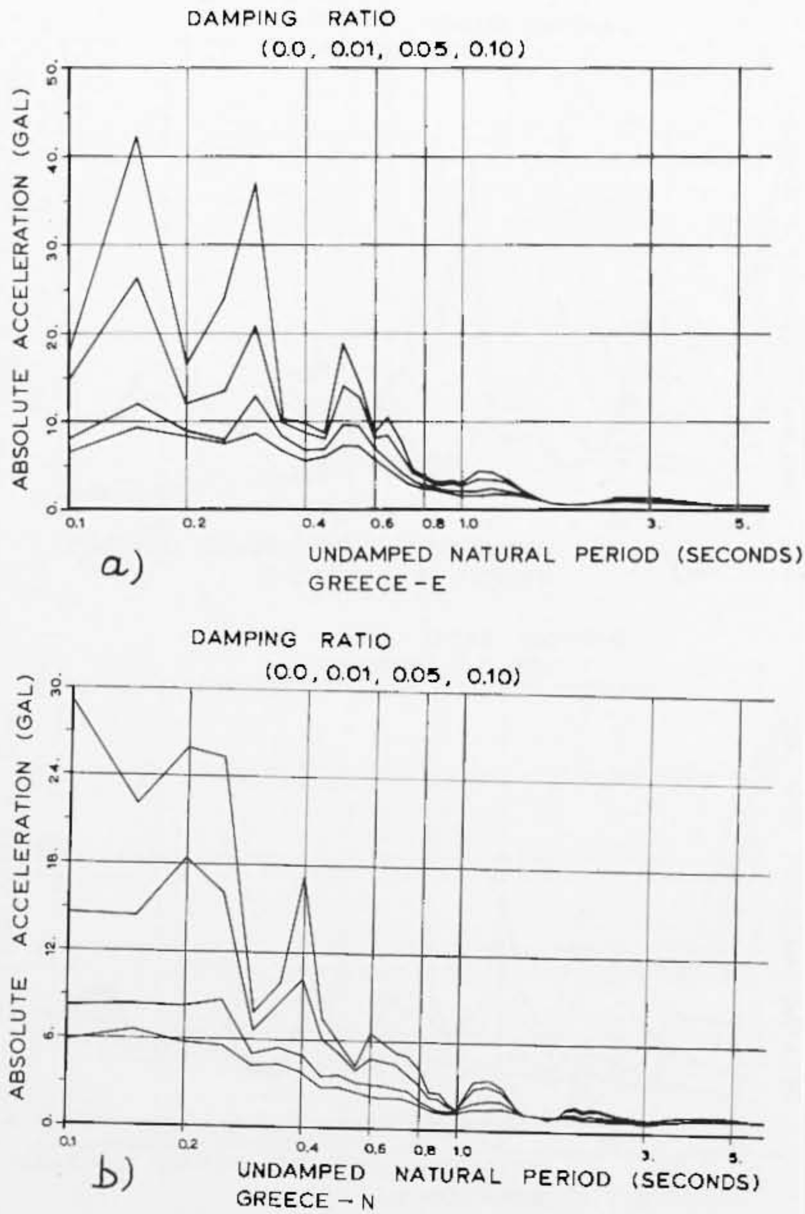

Fig. 13 – Absolute accelerations versus period and different damping ratios of the main shock for E-W (13a) and N-S (13b) components.

curacy we applied the least-mean-square-velocity technique which was introduced by Berg and Housner (1). This technique makes the mean square value of the ground velocity a minimum.

Some useful information about the nature of the motion of the ground have been taken from the main seismic characteristics such as: period-frequency analysis, probability density distribution, autocorrelation function, power spectral density, ground acceleration, velocity and displacement, response spectra etc.

8. – Acknowledgements

The authors are very grateful to prof. A. G. Galanopoulos, University of Athens, for encouragement and for providing the necessary facilities to carry out the present investigation.

REFERENCES

(1) Berg G. and Housner G. W., 1961. – *Integrated velocity and displacement of strong earthquake ground motion.* "Bul. Seism. Soc. Am.", **51**, 2, 175-189.

(2) Brady A. G., 1966. – *Studies of response to earthquake ground motion.* "California Inst. of Technology", Pasadena, California.

(3) Hudson D. E., 1962. – *Some problems in the application of spectrum techniques to strong motion earthquake analysis.* "Bul. Seism. Soc. Am.", **52**, 2, 417-430.

(4) Hudson D. E., 1971. – *Strong motion instrumental data of the San Fernando earthquake of February 9, 1971.* "Earth. Eng. Res. Lab. California Inst. of Technology and Seism". Field Survey of the National Oceanic and Atmospheric Administration.

(5) Hudson D. E., 1972. – *Strong motion Seismology.* "Proceed. of the Intern. Conference on Microzonation", Seattle, USA, Vol. 1, 29-60.

(6) Roussopoulos A., 1971. – *Response analysis of strong motion earthquakes.* Thesis subm. to the Imperial College of Science and Techn. for D.I.C. in Eng. Seismology, 1-128.

(7) Trifunac M. D., 1971. – *Zero base-line correction of strong motion accelerograms.* "Bul. Seism. Soc. Am.", **61**, 5, 1201-1211.